Available online at www.sciencedirect.com
ScienceDirect
Procedia Engineering 2 (2010) 2095–2102
Procedia Engineering
www.elsevier.com/locate/procedia

Fatigue 2010

Fracture mechanics of the three-dimensional crack front: vertex singularity versus out of plain constraint descriptions

Pavel Hutař[a,]*, Martin Ševčík[a,b], Luboš Náhlík[a,b], Michal Zouhar[a,b], Stanislav Seitl[a], Zdeněk Knésl[a], Alfonso Fernández-Canteli[c]

[a]*Institute of Physics of Materials, Academy of Sciences of the Czech Republic, Žižkova 22, 616 62 Brno, Czech Republic*
[b]*Brno University of Technology, Faculty of Mechanical Engineering, Technická 2, 616 69 Brno, Czech Republic*
[c]*University of Oviedo, Department of Construction and Manufacturing Engineering, Campus de Viesques, 33203 Gijón, Spain*

Received 4 March 2010; revised 10 March 2010; accepted 15 March 2010

Abstract

The effect of a free surface on stress distribution along the three-dimensional crack front is discussed. Generalized stress intensity factor methodology and out-of-plane constraint based procedure are used for a reliable estimation of the stress state in front of the crack tip. The two present methodologies are discussed and compared. The out-of plane, in-plane constraint parameters and generalized stress intensity factor were estimated. It is shown significant changes of the singularity exponents and fracture parameters values close to the free surface. Therefore, conventional methodologies can lead to inaccurate description of the stress state and cannot be used for reliable description of fatigue crack propagation in this area.
© 2010 Published by Elsevier Ltd. Open access under CC BY-NC-ND license.
Keywords: in-plain constraint, out of plain constraint, vertex-singularity, linear elastic fracture mechanics

1. Introduction

The fracture mechanics description of the three-dimensional crack front was intensively studied in different works [1,2,3,4]. The main problem is description of the area close to the free surface, where the stress field is more complicated than in the center region. Usual fracture mechanics description of the stress field in the linear elasticity is based on stress intensity factor, which is related to square-root stress singularity. This concept is generally valid and has been used with success several decades, especially for structures where the plain strain conditions prevail. However, in the case of thin structures or in the area close to the free surface this simple description fails and it is necessary generalized usually used concept. Generally, the problem can be solved by two ways. A first stress description can be generalized using vertex singularity. A second possible description is based on out-of plain constraint concept. Both approaches explain more or less the same effect using different methodologies.

* Corresponding author. Tel.: +420 532 290 351
E-mail address: hutar@ipm.cz

1877-7058 © 2010 Published by Elsevier Ltd. Open access under CC BY-NC-ND license.
doi:10.1016/j.proeng.2010.03.225

Over the last 30 years a number of papers which address various aspects of the influence of vertex singularity on the crack behaviour has been published, e.g.[3,4,5,6]. The three-dimensional singular stress field near the point where the crack front intersects the free surface (vertex point) of an elastic body was already investigated by Bažant and Estenssoro [7], Benthem [5], Ghahremani [8]. Using separation variables technique or variation principle, Benthem and Bažant showed that the stress singularity exponent induced by the free surface can be found resulting in power of the singularity weaker than the classical value of 0.5. As a result, the singularity exponent induced by the free surface differs from 0.5 and depends on Poisson's ratio ν of material. Following the literature, the singularity exponent in the vertex point varies between 0.5 (corresponding to $\nu = 0$) and 0.33 (corresponding to $\nu = 0.5$). Despite the intensive effort performed to describe the stress distribution around the vertex singularity by a combination of analytical and numerical methods little has been done to explain the crack behaviour near the free surface from the perspective of fracture mechanics. The methodology based on generalized stress intensity factor, able to describe the crack behaviour close to the free surface, was proposed recently by Hutar et al., see [9,10].

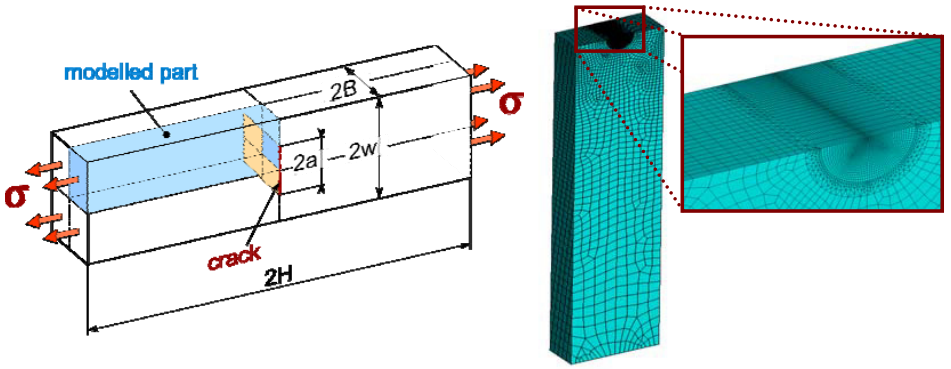

Fig. 1. Schematic MT specimen (left) and preview of finite element mesh used for numerical calculations (right)

The stress description around the 3D crack front based on out of plane constraint is proposed e.g. by Guo et al., see [11,12] or Fernandez-Canteli et al. [13]. The former proposed different descriptions of the stress field as a function of the in-plane constraint (given by T-stress) and out of plane constraint (given by T_z) focused mainly on fracture toughness aplication. The latter proposed description of the singular stress field around crack front by means of expression:

$$\sigma_{ij}(z;r;\theta;B) = \frac{h_{ij}(z;\theta;B)}{\sqrt{2\pi r}} + t_{ij}(z;B) \tag{1}$$

were $h_{ij}(z;\theta;B)$ represents stress intensity tensor and $t_{ij}(z;B)$ constraint tensor. To prove quality of the different descriptions of the stress field the numerical simulations of the middle-crack tension MT specimen (see Fig.1.) were performed and three different approaches for stress field description were compared. Finally, possible usage of the proposed methodologies is discussed. The aim of the present contribution is to discuss and compare different approaches for assessment of 3D character of stress field caused by the existence of body free surfaces. The consequences of stress field changes in the region near the free surface on fatigue crack propagation are then considered.

2. Finite element modeling

The numerical simulations were performed using finite element method software package ANSYS. The tension specimens of length $2H$ = 200mm, width $2w$ = 50mm and thicknesses $2B$ = 2 and 20mm were loaded by applying a uniform stress on the top, see Fig.1. This geometry corresponds to MT specimens used for fatigue crack growth

testing. The 20-nodes iso-parametric elements SOLID 95 with quadratic base-function were used for mesh generation, whereas a very fine mesh was used in the region around the crack front to achieve precise results. Making advantage of the existing symmetry, only one-quarter of the specimen was modeled. A constant Young's modulus E = 200 GPa was assumed throughout while the Poisson's ratio ν was varied between 0 and 0.49 to study its influence. The applied loading stress was considered to be equal to σ = 100MPa. The linear elastic fracture mechanics conditions were assumed to study stress distribution along the crack front.

3. Stress distribution at the crack front

The knowledge of the stress distribution in the crack vicinity is crucial for the assessment of the crack behaviour. Usually, the stress description around the crack tip is characterized by means of one (K) or two (K,T) fracture parameters, which are found to be representative for whole crack front. In general, the effect of the free surface on the stress distribution along the crack front is strong so that local fracture parameters have to be introduced.

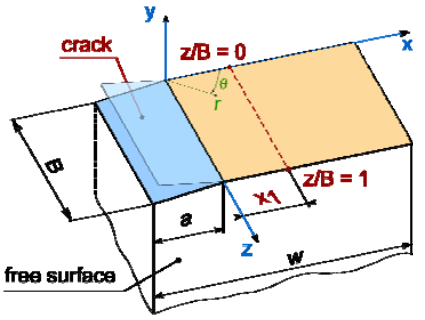

Fig. 2. Cartesian and polar coordinate system on the crack front

Conventionally, the asymptotic stress field σ_{ij} ahead of a crack tip in a homogenous isotropic material under mode I (opening mode) loading, is expressed as:

$$\lim_{r\to 0}\sigma_{ij}^{(I)} = \frac{K_I}{\sqrt{2\pi r}} f_{ij}^{(I)}(\theta) + T_{ij}\delta_{1i}\delta_{1j} + O_{ij}, \tag{2}$$

where K_I is the stress intensity factor, T_{ij} is T-stress, $\delta_{i,j}$ is Cronecker delta, O_{ij} covers all higher terms of Williams expansion, r and θ are polar coordinates, $f_{ij}(\theta)$ is a dimensionless function of the polar angle θ, see Fig. 2. Accordingly, the singular stress distribution for loading mode I in each single layer perpendicular to the crack front is described by the stress intensity factor [14]:

$$\begin{Bmatrix}\sigma_{xx}\\ \sigma_{yy}\end{Bmatrix} = \frac{K_I}{\sqrt{2\pi r}}\begin{Bmatrix}\cos(\theta/2)\left[1-\sin(\theta/2)\sin(3\theta/2)\right]\\ \cos(\theta/2)\left[1+\sin(\theta/2)\sin(3\theta/2)\right]\end{Bmatrix}, \tag{3}$$

whereas σ_{zz} is *0* for plane stress conditions and $\nu(\sigma_{xx}+\sigma_{yy})$ for plane strain conditions. For comparison with this classical stress description, the tensor approach proposed by [13] is considered, in which a new expression for the constant term is used. Assuming validity of the Williams expansion, also for the out-of-plane component σ_{zz}, the stress distribution becomes:

$$\begin{Bmatrix}\sigma_{xx}\\ \sigma_{yy}\\ \sigma_{zz}\end{Bmatrix} = \frac{K_I}{\sqrt{2\pi r}}\begin{Bmatrix}\cos(\theta/2)\left[1-\sin(\theta/2)\sin(3\theta/2)\right]\\ \cos(\theta/2)\left[1+\sin(\theta/2)\sin(3\theta/2)\right]\\ 2\nu\cos(\theta/2)\end{Bmatrix} + \begin{Bmatrix}T_{xx}\\ 0\\ E\varepsilon_{zz}+\nu T_{xx}\end{Bmatrix}, \tag{4}$$

where z is the location in the out-of-plane direction, see Fig. 2, Txx is the in-plane constraint, i.e., the conventional T-stress, and □zz is the out-of-plane normal strain. As a result, the stress state along the crack front is described by three fracture parameters, KI, Txx, Tzz so that Eq. (4) can be used, presumably, to reproduce more precisely the crack behaviour under failure conditions.

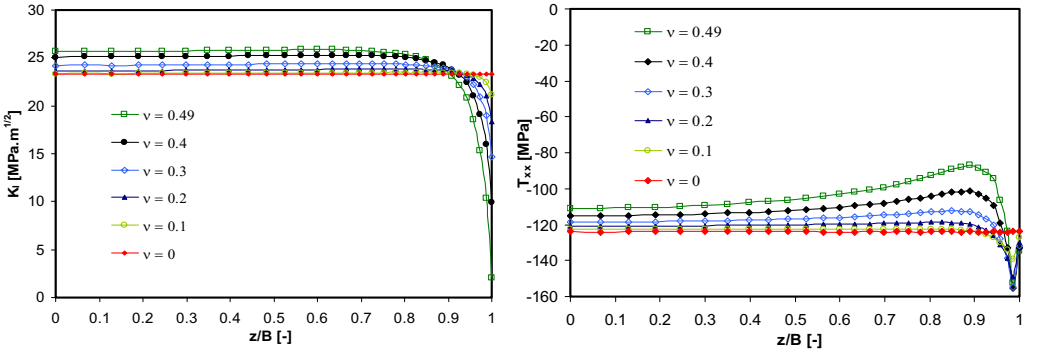

Fig. 3. Stress intensity factor K_I and T-stress (T_{xx}) estimated using the direct method

From the other part, the complicated stress state close to the free surface is the result of a change in the singularity at the vertex point, see e.g. [4,7]. In fact, for a straight crack front and semi-infinite three dimensional body, the stress singularity exponent in the vertex point is found to be weaker than 0.5 and depending on particular value of Poisson's ratio [5,7]. The value of the singularity exponent changes continuously from the central part of the crack to the free surface, and can be estimated using a 3D numerical calculation [6,9]. A methodology, based on the generalized stress intensity factor, which takes into account the change of the stress singularity exponent close to the free surface, was proposed by Hutar et al. [10] allowing the stress distribution to be expressed as:

$$\sigma_{ij} = \frac{H_I}{\sqrt{2\pi}} r^{-p} f_{ij}(\theta, p), \tag{5}$$

where H_I is the generalized stress intensity factor, p is the exponent of the vertex singularity and f_{ij} is a known function. A detailed description of this approach is given in [10].

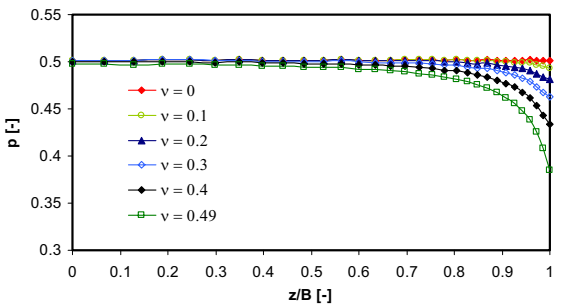

Fig. 4. Vertex singularity exponent along the crack front for different values of the Poisson's ratio

4. Results and discussion

4.1. Estimation of the stress intensity factor, T-stress and exponent of the vertex singularity

Numerical calculations were performed to achieve an accurate description of the stress field σ_{ij} as a function of out-of-plane position z/B (see Fig. 2.). The first task comprised an estimation of the stress intensity factor $K_I(z/B)$ and the T-stress $T_{xx}(z/B)$ along the crack tip for a crack size ratio $a/w = 0.5$. The stress intensity factor, the T-stress and the stress singularity exponent were estimated using the direct method. For this purpose, a specimen thickness of $2B = 20$ mm was considered, and $K_I(z/B)$ and $T_{xx}(z/B)$ were calculated for different Poisson's ratios ranging from $\nu = 0$ to 0.49. The results are shown in Fig. 3.

A drastic change for both K_I and T_{xx} is observed when the position at the crack front is approaching to the free surface of the specimen. This change is greater for increasing Poisson's ratio. The results shown correspond to those published in [6]. Generally, the value of the stress intensity factor decreases while the T-stress increases when approaching to the free surface. The variation experienced by the singularity exponent along the crack front for a specimen thickness of 20 mm and a Poisson's ratio in the range $0 \div 0.5$ is shown in Fig. 4. The singularity exponent varies along the crack front being close to 0.5 in the middle of the specimen ($z/B \cong 0$) while takes the value according to Bažant [7] and Benthem [5] in the point where the crack front intersects the free surface. For $\nu = 0$, the crack stress distribution coincides with that resulting for the classical two-dimensional solution thus being defined simply by K_I, even also in the vertex point. For increasing Poisson's ratio, the singularity exponent decreases in the region influenced by the vertex varying between 0.37 and 0.5, see Fig. 4.

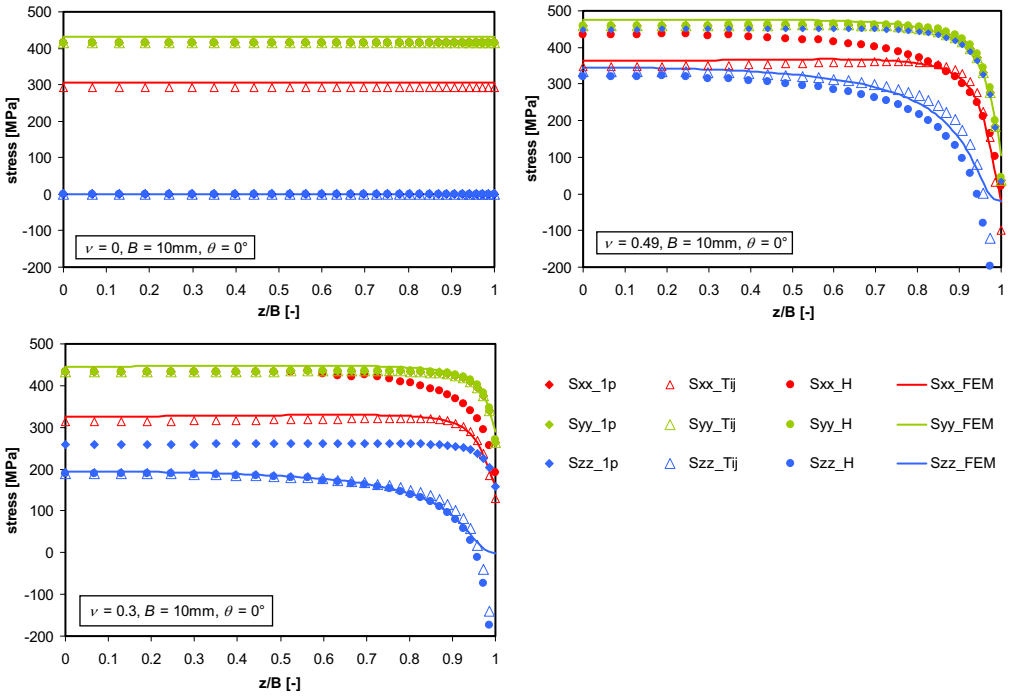

Fig. 5. Stress distribution along the crack front for a specimen thickness $B = 20$ mm and different Poisson's ratios ν. The stress distribution near the crack tip under loading mode I – thick specimen

With the aim of determining the limiting position of some approaches, numerical calculations of the stresses for the plane $\theta = 0°$ near the crack front were performed. A specimen thickness $2B = 20$ mm was assumed throughout. Since materials with a Poisson's ratio $\nu \cong 0.3$ are often used in engineering applications, the subsequent simulations were performed for $\nu = 0.3$ and then compared with the results obtained using Poisson's ratios $\nu = 0$ and $\nu = 0.49$. The effect of the Poisson's ratio on the stress distribution along the crack front for the position $x_1 = 0.5$ mm (see Fig. 2) by thick specimens is depicted in Fig. 5. S_{ij}_1p are the stresses obtained for a one-parameter linear elastic fracture mechanics computed using Eq. (3), $S_{ij}\_T_{ij}$ are the stresses obtained by including the T-stress T_{xx} and T_{zz}, (Eq. (4)) according to [13], S_{ij}_H are the stresses computed by using the generalized stress intensity factor H (Eq. (5)) and, finally, S_{ij}_FEM are the stresses resulting from the application of the finite element method (FEM).

4.2 Stress distribution near the crack front under loading mode I for a thick specimen

In the case of a Poisson's ratio $\nu = 0$, all the referred methods render practically the same stress values these being constant throughout the specimen thickness. For $\nu = 0.49$, a rapid decrease of all stresses is noticed as a result of the deformation induced by the free surface while for $\nu = 0.3$ the stresses are more or less similar to those resulting for $\nu = 0.49$. In the following, the results obtained from standard finite element method simulations are compared with those calculated using the above mentioned approaches. All the methods provide very accurate results for the opening stress σ_{yy} for all the three Poisson's ratios considered. However, the values of the stresses σ_{xx} and σ_{zz} differ substantially. The differences seem to be due to the presence of the T-stress, which in the case of MT specimen influences significantly the values of the σ_{xx} and σ_{zz} stress components. While the stress σ_{zz} in the case of the one-parameter approach differs significantly from the FEM solution, both the approach proposed in [13] and the generalized stress intensity approach are in good agreement even for higher values of Poisson's ratio until the position $z/B \leq 0.95$ where they fall to, apparently, unrealistic negative values. When analyzing the σ_{xx} stresses we observe that only the approach proposed in [13] is almost identical with the FEM solution. Note that for $\theta = 0°$ both stresses σ_{xx} and σ_{yy} coincides in the one-parameter approach because the known function is $f_{ij}(\theta) = 1$.

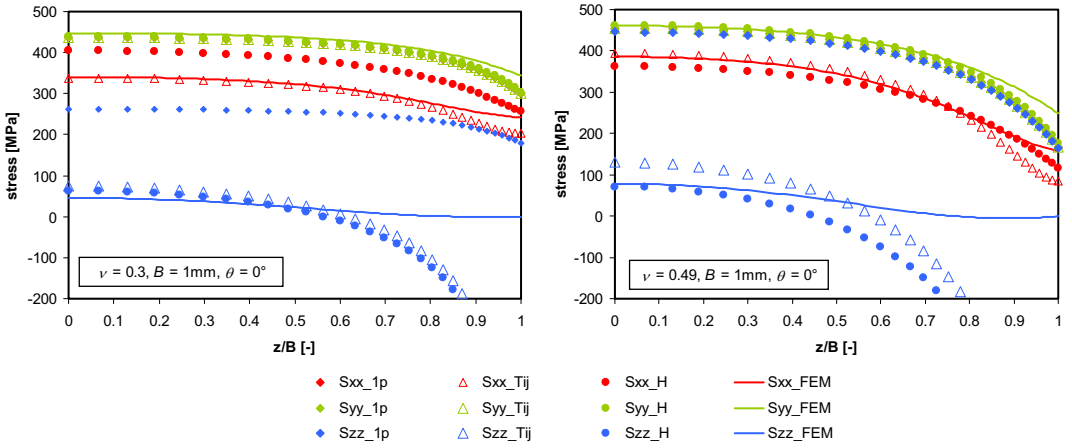

Fig. 6 Stress distribution along the crack tip for various Poisson's ratios ν and thin specimen

4.3 Stress distribution near the crack tip under loading mode I for a thin specimen

For a comparison to Subsection 4.2, where the stress distribution for a thick specimen of thickness $2B = 20$ mm was analyzed, new simulations were performed for a specimen of thickness $2B = 2$ mm with the aim of determining how precisely the stress distribution are described by equations (3), (4) and (5) in the case of thin specimens. The

effect of the Poisson's ratio on the stress distribution in front of the crack tip for thin specimens is presented in Fig. 6.

Both σ_{xx} and σ_{yy} distributions are well described for both values of Poisson ratio using the approach proposed in [13], which loose accuracy when approaching to the free surface, represents the best one of studied methods. When calculating σ_{zz} , the latter approach supplies good solutions only in the middle of the specimen, i.e., for $z/B \approx 0.5$. The one-parameter approach provides only a reliable calculation of $\sigma_{yy.}$ The distribution of the other stress components is inaccurate. The generalized stress intensity factor approach gives similar results to those provide by [13] but it is less precise.

5. Conclusions

The goal of the presented work was to compare three basic approaches for calculating the stress distribution in front of the crack tip in both thick and thin specimens. To this aim MT specimens with two different thickness, 2 mm and 20 mm, were considered. The applied methods consisted of: (i) the classical one-parameter approach based only on stress intensity factor; (ii) a three-parameter approach based on both the in-plane T-stress T_{xx} and the out-of-plane stress T_{zz}; and (iii) the approach based on generalized stress intensity factor H_I.

Using FEM simulations, the stress intensity factor, the T-stress and the exponent of the vertex singularity were estimated and used as an input for the semi-analytical expressions described in Section 3. The stresses $\sigma_{xx,}$ σ_{yy} and σ_{zz} were then calculated along the crack front and compared each other. It can be concluded that the approach suggested in [13] taking T_{xx} and T_{zz} into account was found to be the most proper for both thick and thin specimens. In spite of the fact that for positions of the crack front closer to the free surface this approach supplies results which are not generally accurate, it seems to be the most recommendable. Though the methodology based on the generalized stress intensity factor can be used, especially in the case of thin specimens, a description of the behavior of the fatigue crack requires finding out the relation between K_I, T_{xx}, T_{zz} or H_I and the fatigue crack propagation in the form of the modified Paris' law. This relation, based on Sih's strain energy density concept, can be found, for example, in [10]. The proposal discussed and the results found can explain the effect of the free surface on the fatigue crack behavior in the framework of the linear elastic fracture mechanics allowing us to assess the influence of the 3D stress field character on fatigue crack shape and propagation, thus contributing towards a more reliable estimation of the residual fatigue lifetime for thin-walled structures.

Acknowledgement

This work was supported by Czech Science Foundation through grants no. 101/09/0867, 106/09/1954 and by AS CR project no. M100410901. Partial support given by DGICYT of the Spanish Ministry of Science and innovation (Project DPI2007-66903 and by FICYT (Project IB08-171) is also acknowledged.

References

[1] Olaosebikan L. On the variation of stress along the front of cracks and surface flows. *Engineering Fracture Mechanics* 1990;**37**:221-235.

[2] Heyder M, Kolk K, Kuhn G. Numerical and experimental investigations of the influence of corner singularities on 3D fatigue crack propagation. *Engeneering Fracture Mechanics* 2005;**75**;2095-2105.

[3] Kotousov A, Fracture in plates of finite thickness. *International Journal of Solids and Structures* 2007;**44**;8259-8273.

[4] Pook LP, Some implications of corner point singularities. *Engineering Fracture Mechanics* 1994;**48**:367-378.

[5] Benthem JP, State of stress at the vertex of a quarter-infinite crack in half-space. *International Journal of Solids and Structures* 1977;**13**;479-492.

[6] de Matos PFP, Nowell D. Numerical simulation of plasticity-induced fatigue crack closure with empasis on the crack growth scheme 2D and 3D analyses. *Engineering Fracture Mechanics* 2008;**75**:2087-2114.

[7] Bažant ZP, Estenssoro LF. Surface singularity and crack propagation. *International Journal of Solids and Structures* 1979;**15**;405-426.

[8] Ghahremani F. A numerical variational method for exacting 3D singularities. *International Journal of Solids and Structures* 1991;**27**;1371-1386.

[9] Hutař P, Náhlík L, Knésl Z. Quantification of the influence of vertex singularities on fatigue crack behavior. *Computational Materials Science* 2009;**45**;653-657.

[10] Hutař P, Náhlík L, Knésl Z. The effect of a free surface on fatigue crack behaviour. *International Journal of Fatigue*, doi:10.1016/j.ijfatigue.2010.01.009.

[11] She Ch, Guo W, The out-of-plane constraint of mixed-mode cracks in thin elastic plates, *International Journal of Solids and Structures* 2007;**44**;3021-3034.

[12] Zhao J, Guo W, Chongmin S. The in-plane and out-of-plane stress constraint factors and K-T-Tz description of stress field near the border of a semi-elliptical surface crack. *International Journal of Fatigue* 2007;**29**;435-443

[13] Fernández-Canteli A, Fernández-Sáez J, Fernández-Zúñiga D. On the T-stress and its influence on constraint due to specimen thickness and crack length under mode-I loading, *12th International Conference on Fracture*, Ottawa, 2009

[14] Anderson TL. Fracture Mechanics: Fundamentals and Applications. 3rd ed. CRC press; 2005